

## Electronic Supporting Information

# Programmable precise kinetic control over crystal phase, size, and equilibrium in spontaneous metathesis reaction for Cs-Pb-Br nanostructure patterns at room temperature

Marek Piotrowski<sup>† [a]</sup>, Zhongsheng Ge,<sup>† [a]</sup> Yixi Wang,<sup>[a]</sup> Anil Kumar Bandela\*<sup>[b]</sup> and Udayabhaskararao Thumu\*<sup>[a]</sup>

\*Corresponding authors: bandela@post.bgu.ac.il and uday@uestc.edu.cn

<sup>[a]</sup>Institute of Fundamental and Frontier Sciences, University of Electronic Science and Technology of China, Chengdu 610054, China. <sup>[b]</sup>Department of Chemistry, Ben Gurion University of the Negev, Beer Sheva 84105, Israel.

[<sup>†</sup>] These authors contributed equally to this work.

### Table of contents

| Serial order | Description                                  | Page no. |
|--------------|----------------------------------------------|----------|
| S1           | Experimental Section & Analytical procedures | 2-3      |
| S2           | Table 1                                      | 2        |

### Supporting Figures

|               |                                                                                                     |       |
|---------------|-----------------------------------------------------------------------------------------------------|-------|
| Figure S1     | Photographs of reaction in $\delta_1$ , $\delta_2$ , and $\delta_3$                                 | 4     |
| Figure S2     | XRD study of mixed CsPbBr <sub>3</sub> and Cs <sub>4</sub> PbBr <sub>6</sub> phases                 | 5     |
| Figure S3&S4  | HAADF-STEM EDS analysis                                                                             | 6&7   |
| Figure S5     | UV-vis spectra: the study of rapid reaction in $\delta_1$                                           | 8     |
| Figure S6     | UV-vis spectra: influence of Cs <sup>+</sup> ions in $\delta_1$                                     | 8     |
| Figure S7-10  | UV-vis spectra: reactions upon the titration in $\delta_1$ to $\delta_3$                            | 9-12  |
| Figure S11    | Study of rapid reaction at $\delta_2$ region by absorption spectra in $\delta_1$                    | 13    |
| Figure S12    | UV-vis spectra in $\delta_3$                                                                        | 14    |
| Figure S13    | Analysis of absorption bands for reactions in $\delta_1$                                            | 14    |
| Figure S14-15 | TEM images of transient state                                                                       | 15    |
| Figure S16    | TEM images of immediate reaction in $\delta_1$                                                      | 16    |
| Figure S17    | TEM images of reaction in lower $\delta_2$ (Cs <sub>4</sub> PbBr <sub>6</sub> )                     | 16    |
| Figure S18    | TEM images of reaction in higher $\delta_2$ (Cs <sub>4</sub> PbBr <sub>6</sub> )                    | 17    |
| Figure S19-20 | TEM images of reaction in higher $\delta_2$ to $\delta_3$ (Cs <sub>4</sub> PbBr <sub>6</sub> -CsBr) | 18    |
| Figure S21    | TEM images of immediate reaction in $\delta_2$                                                      | 19    |
| Figure S22    | TEM images of spherical CsBr NCs in lower $\delta_3$                                                | 19    |
| Figure S23-24 | TEM images of CsBr nanocubes in moderate $\delta_3$                                                 | 20&21 |
| Figure S25    | UV-vis spectra: the study of OA influence                                                           | 22    |
| Figure S26    | TEM images of sharp-edged CsBr nanocubes                                                            | 23    |
| Figure S27    | TEM images of round-edged CsBr nanocubes                                                            | 23    |
| Figure S28    | TEM images of self-assembly of CsBr nanocubes                                                       | 24    |
| Figure S29    | TEM images of larger CsBr nanocubes                                                                 | 25    |
| Figure S30    | Time-dependent PL emission in $\delta_1$ (with solvent)                                             | 25    |
| Figure S31    | Time-dependent PL emission in $\delta_1$ (without solvent)                                          | 26    |
| Figure S32-33 | PL emission: cyclic experiment                                                                      | 27    |
| Figure S34    | TEM images of reaction at $\delta_1$ under ethanol influence                                        | 28    |

## S1-Experimental section

**Chemicals.** Cesium carbonate ( $\text{Cs}_2\text{CO}_3$ ), lead bromide ( $\text{PbBr}_2$ ), octadecene (ODE), oleic acid (OA), and oleylamine (OLAM) were purchased from Sigma-Aldrich. All chemicals were used without further purification.

**Preparation of Cs-oleate ( $\text{P}_{\text{Cs-ol}}$ ):**  $\text{Cs}_2\text{CO}_3$  (0.814 g) was loaded into a 100 mL 3-neck flask along with ODE (40 mL) and OA (2.5 mL), dried for 1 h at 120 °C, and then heated under argon to 150 °C until all  $\text{Cs}_2\text{CO}_3$  reacted with OA. This solution is transferred to a glass vial and used as it is for titration purposes. This reaction solution is labelled as  $\text{P}_{\text{Cs-ol}}$  in the main text.  $\text{P}_{\text{Cs-ol}}$  is known as milky white dispersion in octadecane at RT.

**Preparation of  $\text{PbBr}_2$  precursor ( $\text{P}_{\text{Pb-br}}$ ):** ODE (5 mL) and  $\text{PbBr}_2$  (0.069 g) were loaded into 25 mL 3-neck flask and dried under vacuum for 1 h at 120 °C. OLAM (0.5 mL) and OA (0.5 mL) were injected at 120 °C under argon flow. The transparent colorless ODE is changed to a clear pale-yellow in 10 min of reaction. This reaction solution is labelled as  $\text{P}_{\text{Pb-br}}$  in the text.

**Systematic study of metathesis reaction:** At first, several tens of reaction vials containing a fixed amount, 100  $\mu\text{L}$  of  $\text{P}_{\text{Pb-br}}$  in 2 mL hexane, are prepared. To which microliter quantity (2-300  $\mu\text{L}$  range) of precursor,  $\text{P}_{\text{Cs-ol}}$  was added against  $\text{P}_{\text{Pb-br}}$  solution at RT in a 5 mL vial and shaken at 900 rpm. Each reaction vial was treated individually for spectroscopic and microscopic study. The solution of initial milky white  $\text{P}_{\text{Cs-ol}}$  is directly titrated against  $\text{P}_{\text{Pb-br}}$ , which turned into a clear solution immediately after mixing both the precursors and no sedimentation was found. The quick solubility of  $\text{P}_{\text{Cs-ol}}$  is due to the increased concentration of long-chain OA and OLAM, which are present in the form of complexed  $\text{P}_{\text{Pb-br}}$  in hexane. The presence of all three reacting ions in the same phase quickens (within 2 sec.) the metathesis reaction and spectroscopic changes are clearly observable under all the reaction conditions. The details are listed in Table 1.

**S2-Table 1**

|            | $\text{P}_{\text{Pb-br}} / \text{P}_{\text{Cs-ol}} (\delta)$ | $\text{P}_{\text{Pb-br}}$ [ $\mu\text{L}$ ] | $\text{P}_{\text{Cs-ol}}$ [ $\mu\text{L}$ ] | Crystal structure                | Morphology                                      |
|------------|--------------------------------------------------------------|---------------------------------------------|---------------------------------------------|----------------------------------|-------------------------------------------------|
| $\delta_1$ | Lower $\delta_1$                                             | 100                                         | 2 to 15                                     | $\text{CsPbBr}_3$                | Ultrathin NBs (length:1-3 $\mu\text{m}$ )       |
|            | Moderate $\delta_1$                                          |                                             | 15 to 25                                    |                                  | Nanoplatelets ( 10 nm)                          |
|            | Higher $\delta_1$                                            |                                             | 25 to 40                                    | $\text{CsPbBr}_3$ clusters       | Ultrathin NBs (length: 100 nm)                  |
| $\delta_2$ | Lower $\delta_2$                                             | 100                                         | 45 to 60                                    |                                  | $\text{Cs}_4\text{PbBr}_6$ NCs (length: 100 nm) |
|            | Moderate $\delta_2$                                          |                                             | 62 to 80                                    | $\text{Cs}_4\text{PbBr}_6$       | $\text{Cs}_4\text{PbBr}_6$ NCs (length: 100 nm) |
|            | Higher $\delta_2$                                            |                                             | 80 to 140                                   | $\text{Cs}_4\text{PbBr}_6$ -CsBr | Mixed NCs (10 nm)                               |
| $\delta_3$ | Lower $\delta_3$                                             | 100                                         | 140 to 180                                  |                                  | Spherical CsBr NCs                              |
|            | Moderate $\delta_3$                                          |                                             | 180 to 250                                  | CsBr                             | Cubic CsBr NCs (25 nm)                          |
|            | Higher $\delta_3$                                            |                                             | 250 to 300                                  |                                  | CsBr NCs (50 to 200 nm)                         |

### **Optical characterization.**

- (a) Ultraviolet-visible (UV-vis) absorption spectra were detected with the Shimadzu UV-1900 Spectrophotometer. Around 50 individual reaction vials were prepared as per the details in the previous section (2-300  $\mu\text{L}$  of precursor,  $\text{P}_{\text{Cs-ol}}$  was added against 100  $\mu\text{L}$   $\text{P}_{\text{Pb-br}}$  in 2 mL hexane). From the total volume of each reaction sample containing close to 2 mL, for each absorption measurement, 100  $\mu\text{L}$  of the reaction solution was collected and diluted with 2 mL hexane to measure the absorption at different time intervals (30 min, 4 h, 8 h, 12 h, and 24 h). The reaction was subjected to a constant dilution for all the UV measurements in order to avoid obscuring the display for direct solutions.
- (b) The photoluminescence (PL) was measured using the Hitachi F-4700 fluorescence spectrophotometer. Around 50 individual reaction vials were prepared (2-300  $\mu\text{L}$  of precursor,  $\text{P}_{\text{Cs-ol}}$  was added against 100  $\mu\text{L}$   $\text{P}_{\text{Pb-br}}$  in 2 mL hexane). The total volume of each reaction sample containing close to 2 mL. For each PL measurement, the reaction solution was used as it is without further dilution.

**PL emission cyclic experiment:** That experiment was performed at the  $\delta_1$  region on a larger scale (10 times), where 0.1 ml  $\text{P}_{\text{Cs-ol}}$  is added to a 1 mL  $\text{P}_{\text{Pb-br}}$  in 20 ml hexane mixture and shaken the reaction at 900 rpm. The solution was concentrated at different time intervals (30 min, 1.5 h, 2.4 h, 3.5 h, 6.5 h, and 20 h) specifically for PL measurements. After the PL measurements, necessary hexane was added to the concentrated solution in order to make up to the original volumes.

**Electron microscopy characterization.** Transmission electron microscopy (TEM) measurements were carried out on the JEOL JEM-1400 Flash electron microscope at an acceleration voltage of 120 kV. Energy-dispersive X-ray spectroscopy (EDX) in high-angle annular dark-field scanning TEM mode (HAADF-STEM-EDX) studies were performed on FEI Tecnai G<sup>2</sup> F20 operating at an acceleration voltage of 200 kV.

## Supporting figures

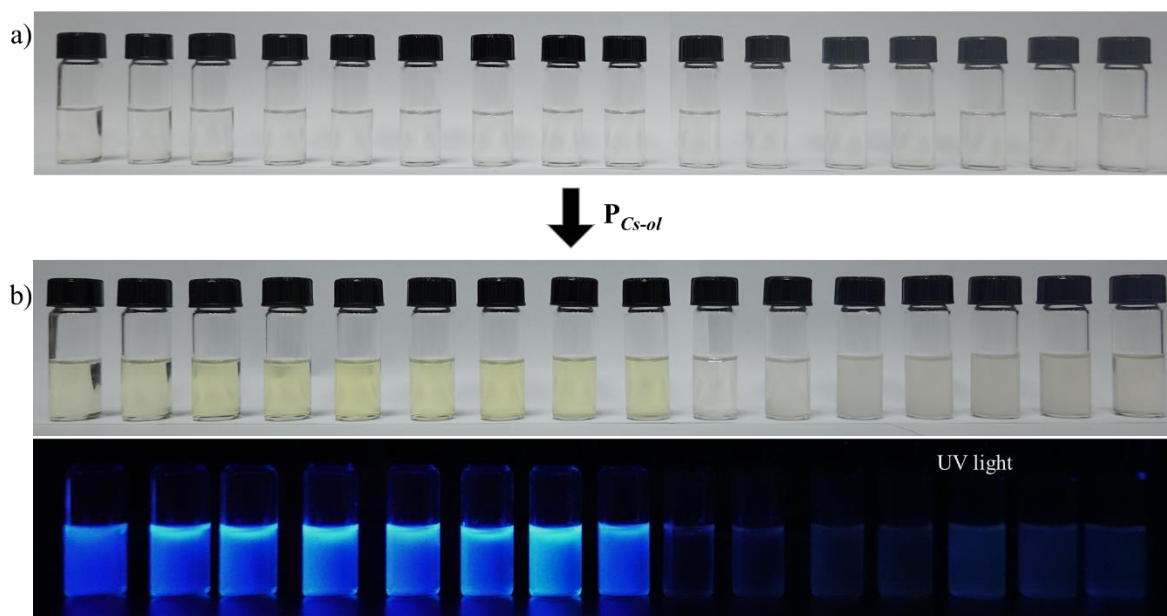


**Figure S1.** The photographs of the RT synthesis of Cs-(Pb)-Br NCs at various amounts of  $P_{Cs-ol}$  against 100  $\mu$ L of  $P_{Pb-br}$ . a) 100  $\mu$ L of precursor,  $P_{Pb-br}$  (in the form of  $PbBr_2$  complexed with OA and OLAM in ODE) in 2 mL hexane. b) selective reaction vial photographs, where 6  $\mu$ L to 200  $\mu$ L (corresponding to  $\delta_1$ ,  $\delta_2$ , and  $\delta_3$ , respectively) of precursor,  $P_{Cs-ol}$  was added to sample, (a) and shaken at 900 rpm for 4 h. (b) and (c) are the photographs of the samples in visible and UV light.

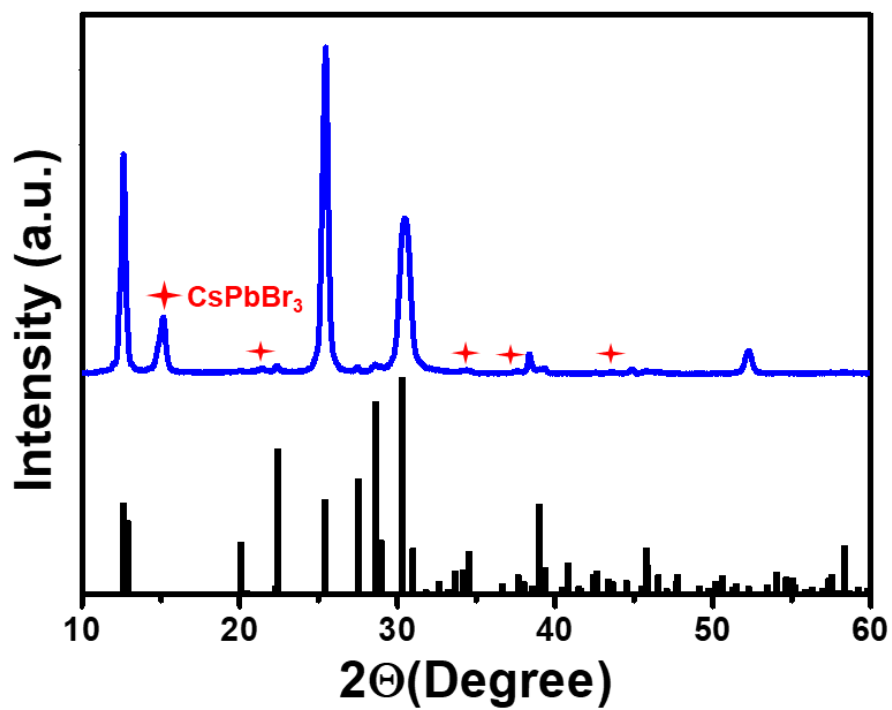


**Figure S2.** X-ray diffraction patterns of the region where the CsPbBr<sub>3</sub> and Cs<sub>4</sub>PbBr<sub>6</sub> are exist together. The “red star” symbol indicates the theoretical diffraction positions of CsPbBr<sub>3</sub>.

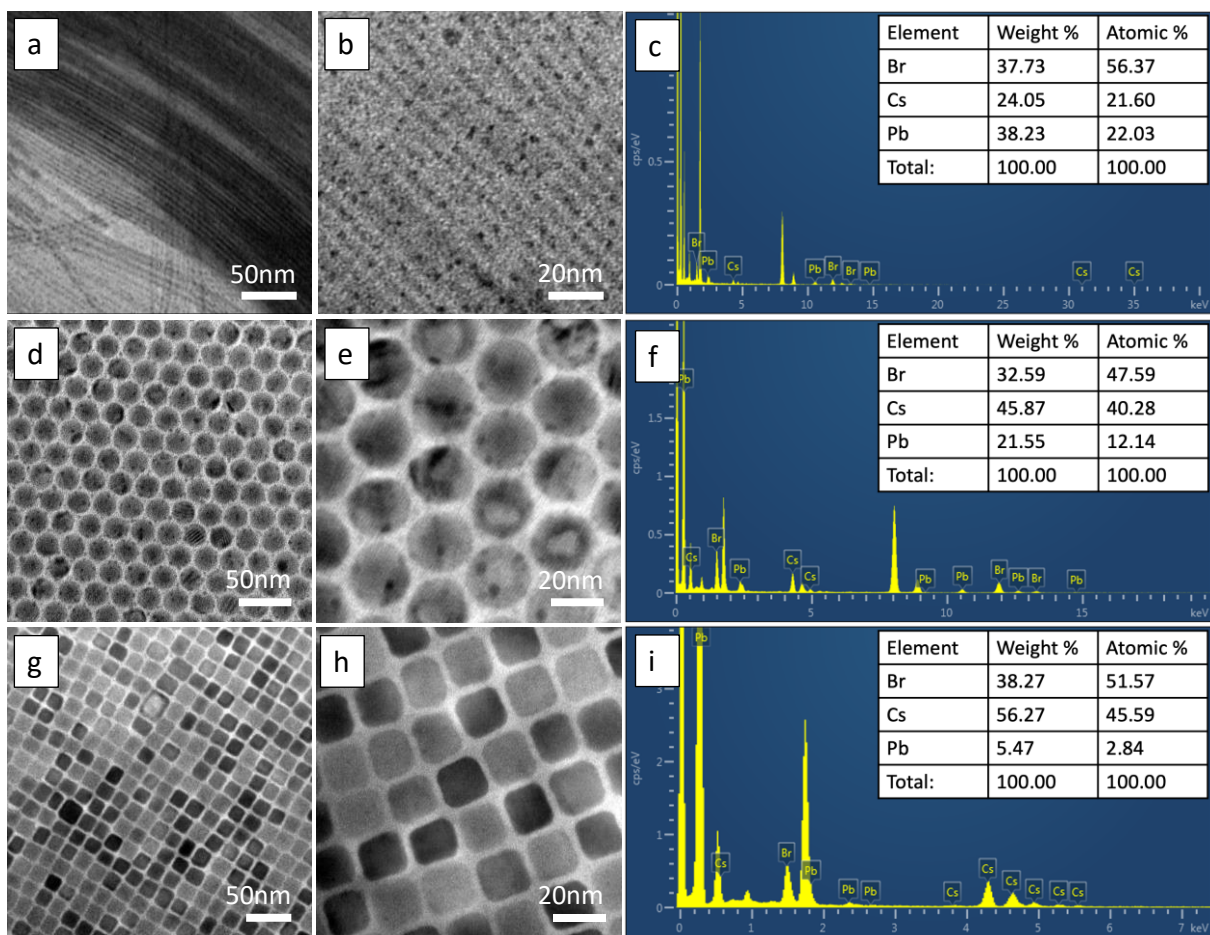


**Figure S3.** Low- and high magnification TEM images of CsPbBr<sub>3</sub> NBs (a, b), Cs<sub>4</sub>PbBr<sub>6</sub> NCs (d, e), and CsBr NCs (g, h) and their respective EDX spectra with Br, Cs, and Pb elemental weight % and atomic % (c, f, and i). The atomic percentages 1:1:2.6, 4:1.2:5 and 1:0.06:1.1 are in good agreement with the three phases CsPbBr<sub>3</sub>, Cs<sub>4</sub>PbBr<sub>6</sub>, and CsBr, respectively. Note that bromine is deficient in the case of CsPbBr<sub>3</sub>, Cs<sub>4</sub>PbBr<sub>6</sub>, and the presence of negligible amounts of Pb presence for CsBr. The slight amounts of Pb cannot be avoided in EDS as the NCs are not subjected to the purification process.

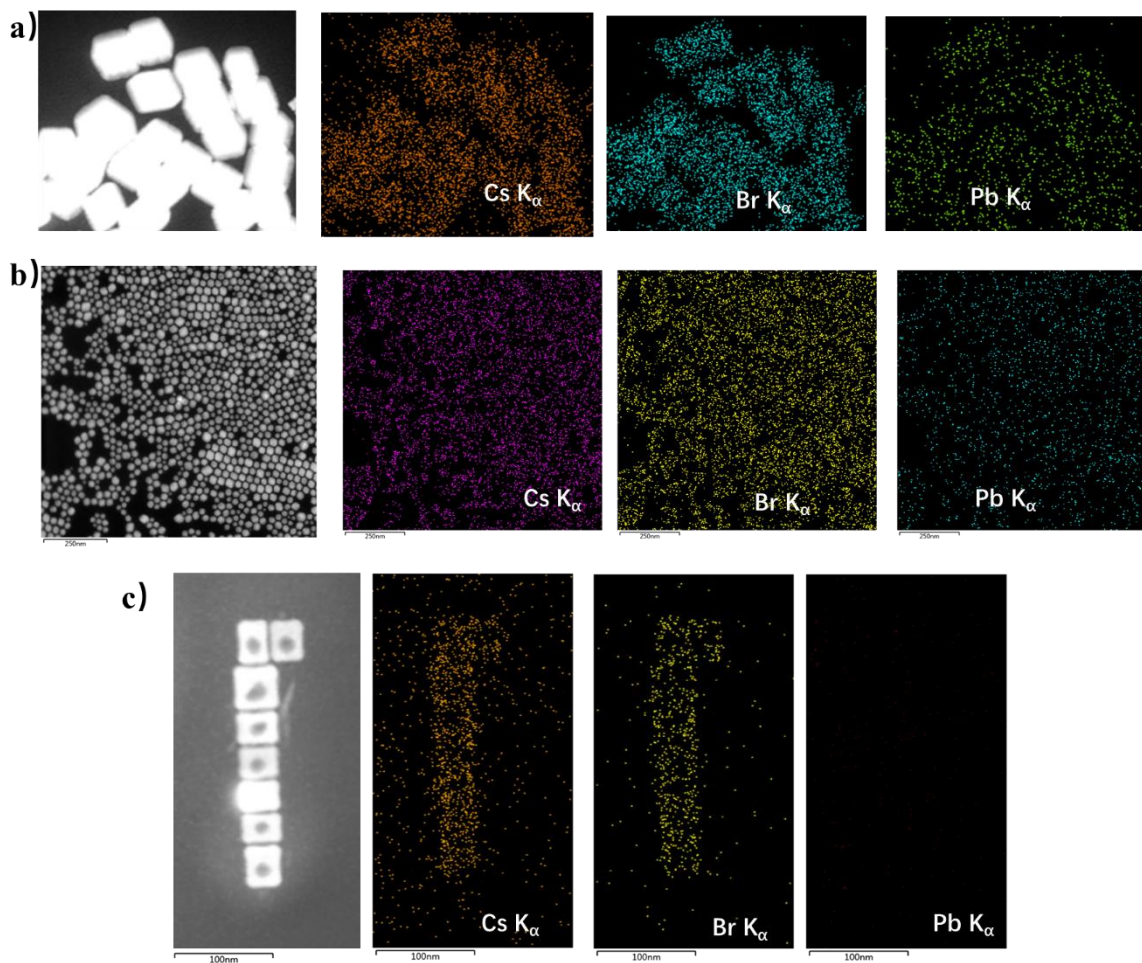


**Figure S4:** SEM image and corresponding EDS elemental mapping of Cs<sub>4</sub>PbBr<sub>6</sub> NCs (100 nm (a), Cs<sub>4</sub>PbBr<sub>6</sub> NCs (15 nm) (b) and cubic CsBr NCs (c).

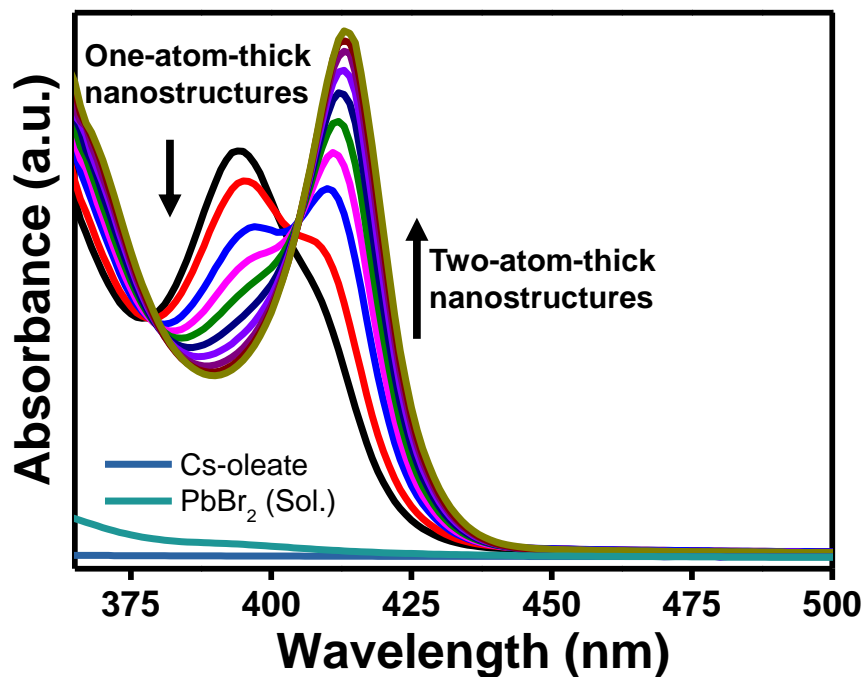


**Figure S5.** Time-dependent absorption spectra collected after 15 min of reaction in the  $\delta_1$  region, where 2  $\mu\text{L}$   $\text{P}_{\text{Cs-ol}}$  is titrated with 100  $\mu\text{L}$   $\text{P}_{\text{Pb-br}}$  for the formation of  $\text{CsPbBr}_3$  nanostructures. Black arrows indicate the transformation of one-monolayer to two-monolayer structures.

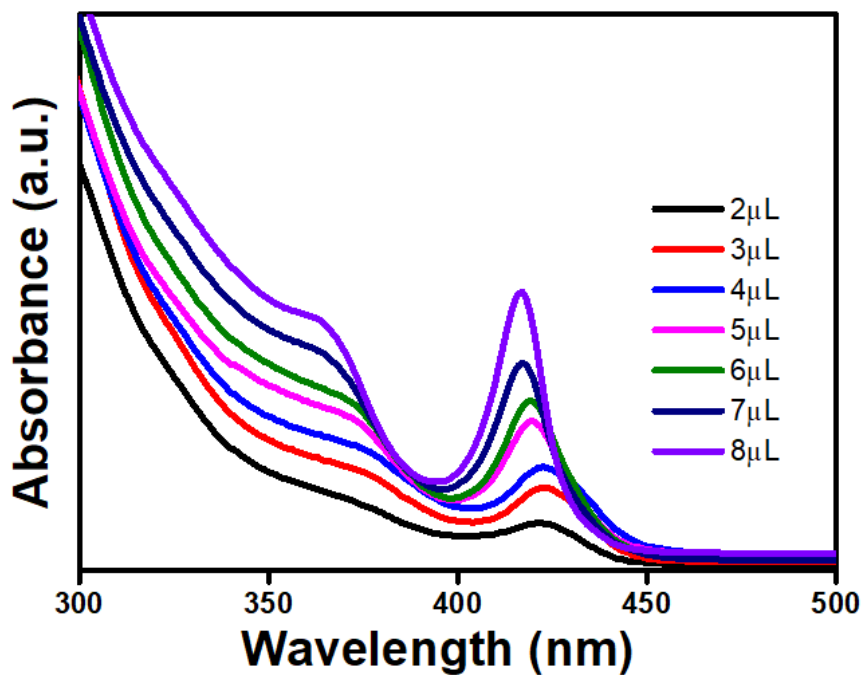


**Figure S6.** Absorption spectra of the reactions collected after 30 minutes of reactions, where 2 to 8  $\mu\text{L}$  of  $\text{P}_{\text{Cs-ol}}$  was titrated against 100  $\mu\text{L}$  of  $\text{P}_{\text{Pb-br}}$ .



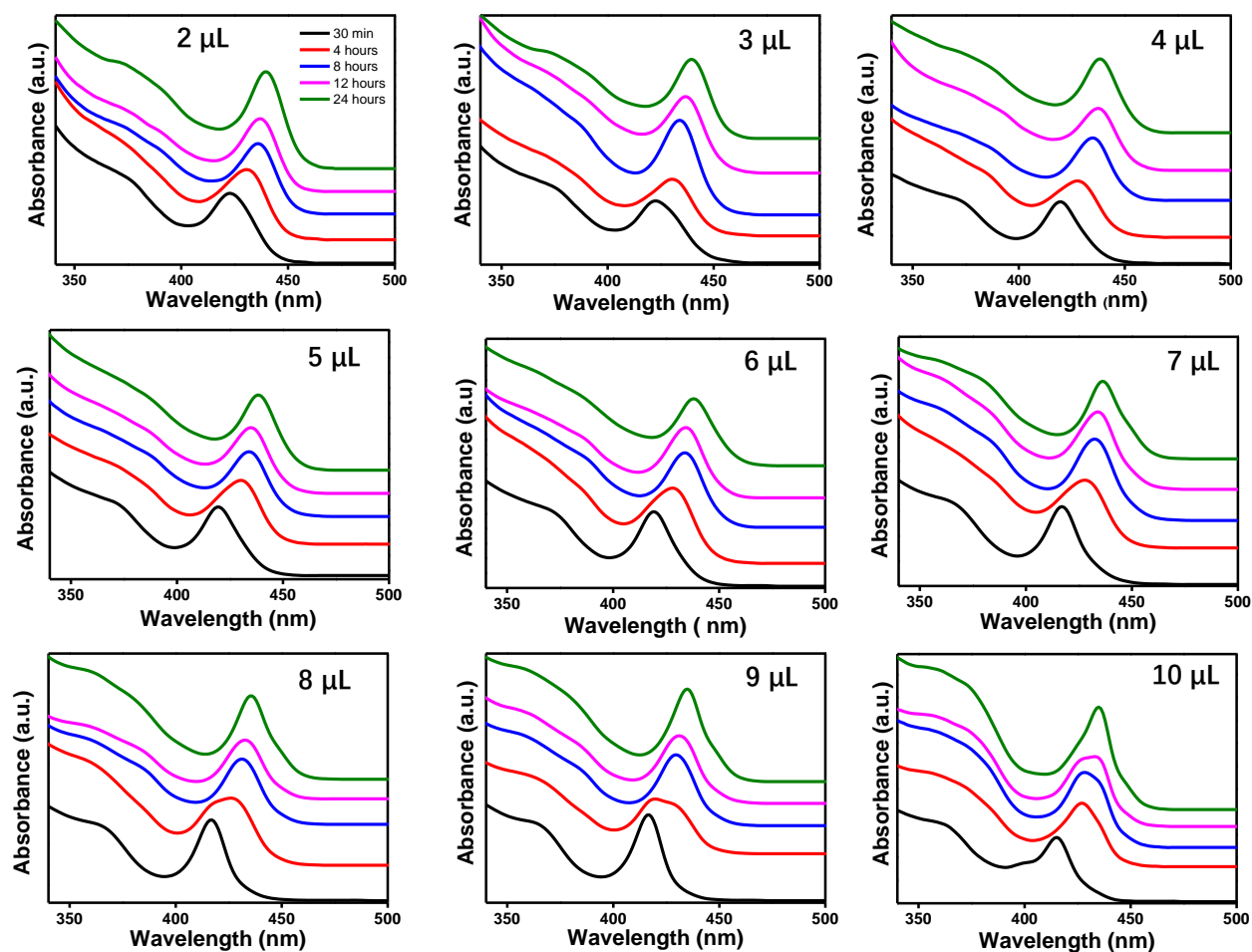


**Figure S7.** Time-dependent absorption spectra of the nanostructures formed upon the titration of  $P_{Cs-ol}$  (starting from 2  $\mu\text{L}$  to 10  $\mu\text{L}$ ) against 100  $\mu\text{L}$  of  $P_{Pb-br}$  in 2 mL hexane. The x-axis is in the range of 340 nm to 500 nm. For clarity, the absorption spectra in each panel are vertically translated. The color code of the graphs represents different time intervals. The black trace represents 30 mins, the red trace for 4 h, the blue trace for 8 h, the pink trace for 12 h, and the green trace indicates 24 h of the reaction. The same color code for different time intervals was used for S8, S9, and S10.

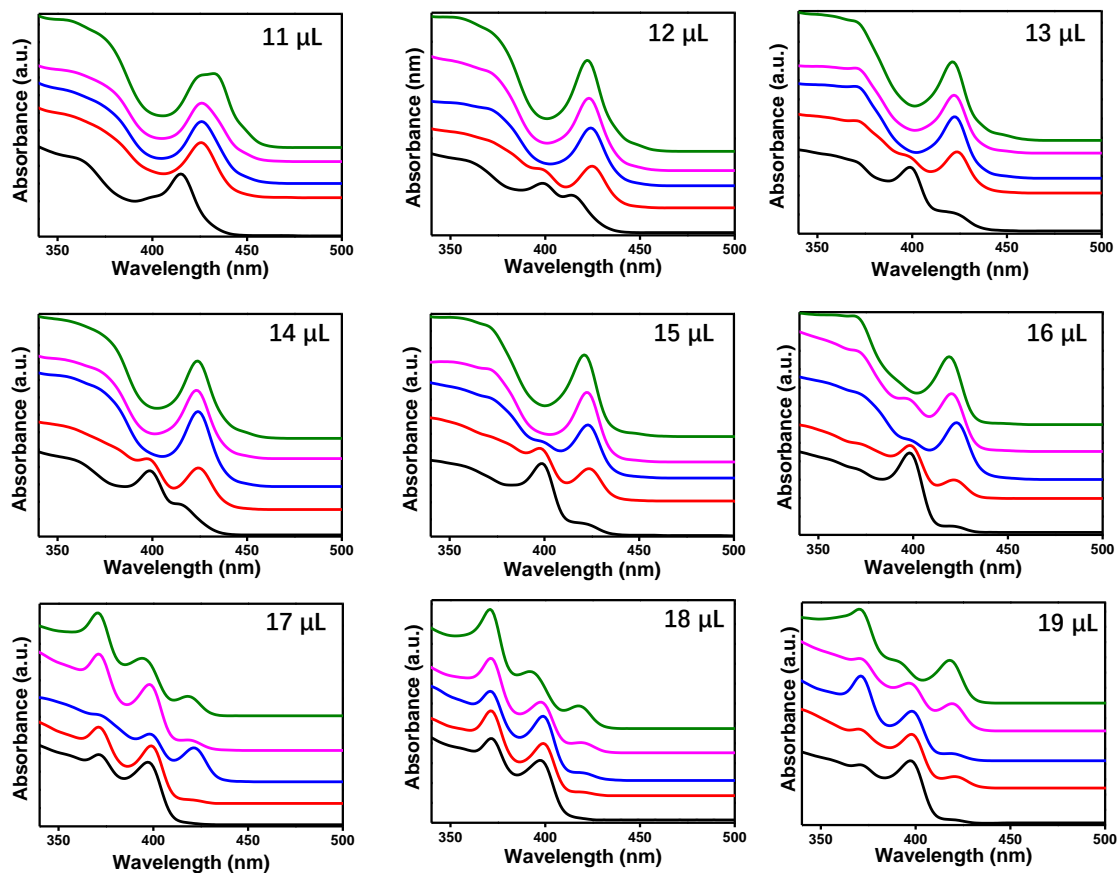


**Figure S8.** Time-dependent absorption spectra of the nanostructures formed upon the titration of  $P_{CS-ol}$  (starting from 11  $\mu\text{L}$  to 19  $\mu\text{L}$ ) against 100  $\mu\text{L}$  of  $P_{Pb-br}$  in 2 mL hexane. The x-axis is in the range of 340 to 500 nm. For clarity, the absorption spectra in each panel are vertically translated. The color code of the graphs represents different time intervals.

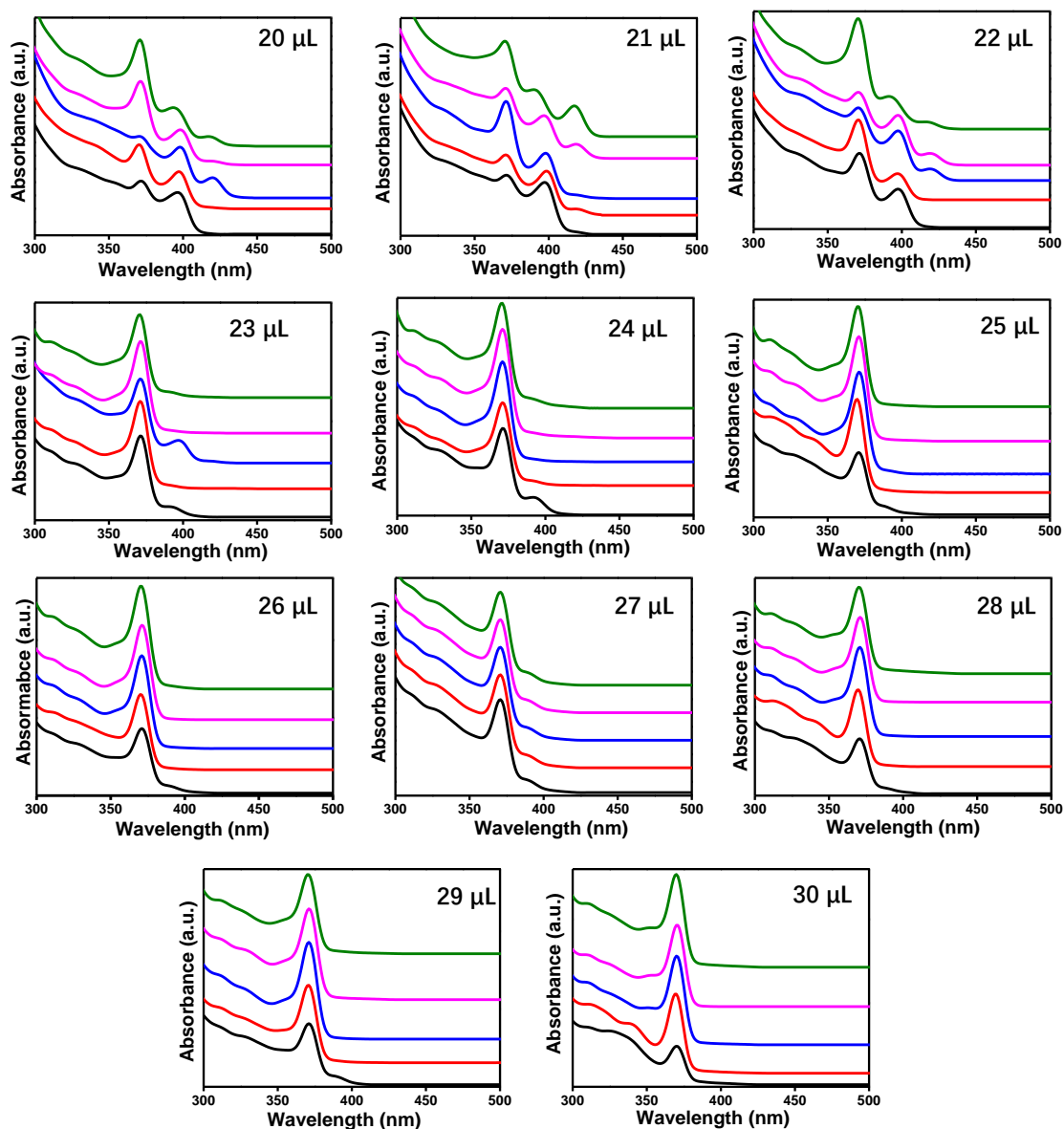


**Figure S9.** Time-dependent absorption spectra of the nanostructures formed upon the titration of  $P_{Cs-ol}$  (starting from 20  $\mu\text{L}$  to 30  $\mu\text{L}$ ) against 100  $\mu\text{L}$  of  $P_{Pb-br}$  in 2 mL hexane. The x-axis is in the range of 300 to 500 nm. For clarity, the absorption spectra in each panel are vertically translated. The absorption peak at 370 nm is relatively stable without any sign of degradation even after 24 h.

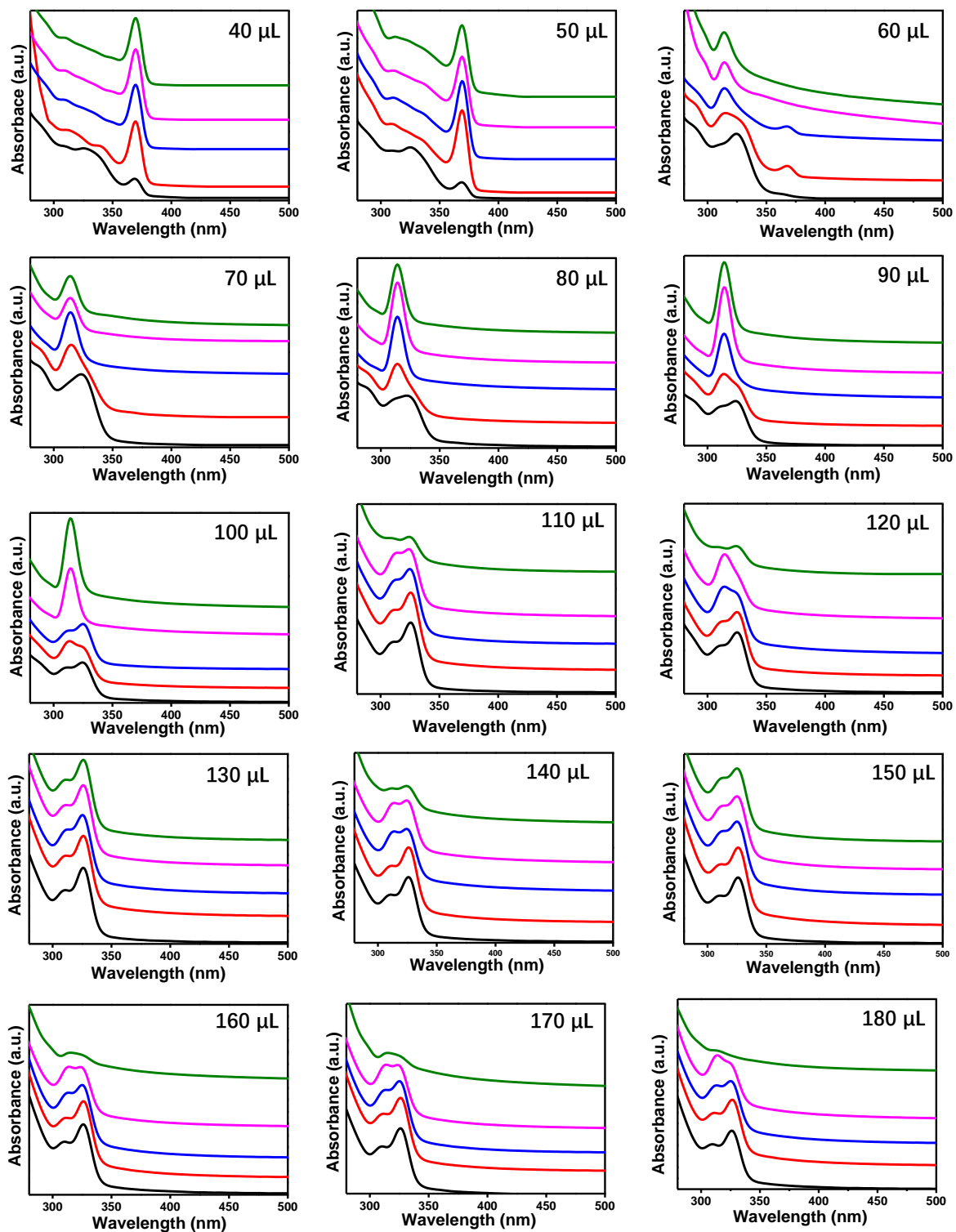


**Figure S10.** Time-dependent absorption spectra of the nanostructures formed upon the titration of  $P_{Cs-ol}$  (starting from 40  $\mu\text{L}$  to 180  $\mu\text{L}$ ) against 100  $\mu\text{L}$  of  $P_{Pb-br}$  in 2 mL hexane. The x-axis is in the range of 340 to 500 nm. For clarity, the absorption spectra in each panel are vertically translated.

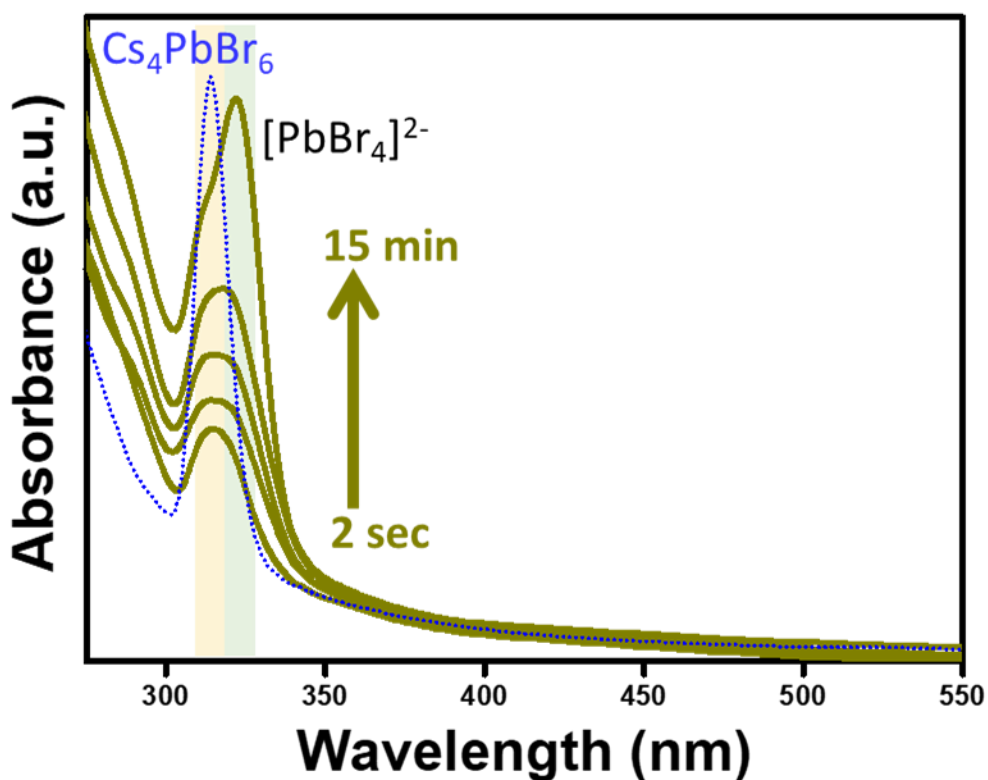


**Figure S11.** Study of rapid reaction at  $\delta_2$  region through time-dependent absorption spectra. The reaction was conducted at the  $\delta_2$  region, where 80  $\mu\text{L}$  of  $\text{P}_{\text{Cs-ol}}$  is titrated against 100  $\mu\text{L}$  of  $\text{P}_{\text{Pb-br}}$ . The upward arrow represents the formation equilibrium state among  $\text{Cs}_4\text{PbBr}_6$  NCs and  $[\text{PbBr}_4]^{2-}$  from 2 seconds to 15 minutes. This equilibrium state was eventually shifted towards the formation of single  $\text{Cs}_4\text{PbBr}_6$  NCs over reaction time, as confirmed by the presence of a single absorption peak at 313 nm (blue trace). The TEM images of  $\text{Cs}_4\text{PbBr}_6$  NCs formed at the time of immediate reaction are given in S21.

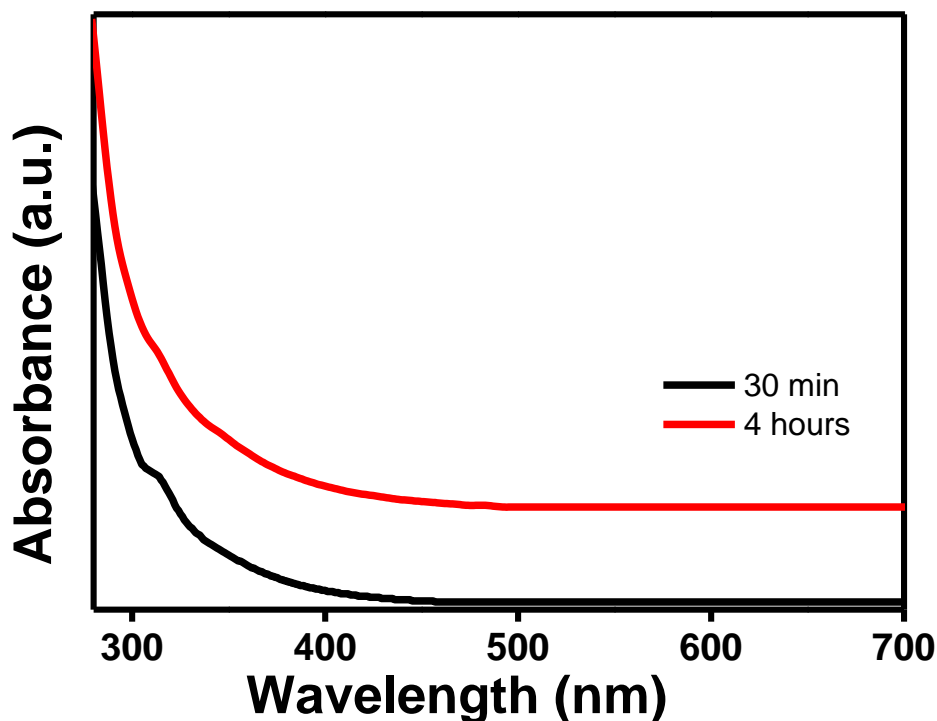


**Figure S12.** Time-dependent absorption spectra of the CsBr NCs formed upon the titration of 250  $\mu\text{L}$  of  $\text{P}_{\text{Cs-ol}}$  against 100  $\mu\text{L}$  of  $\text{P}_{\text{Pb-br}}$  in 2 mL hexane show a nearly featureless spectrum.

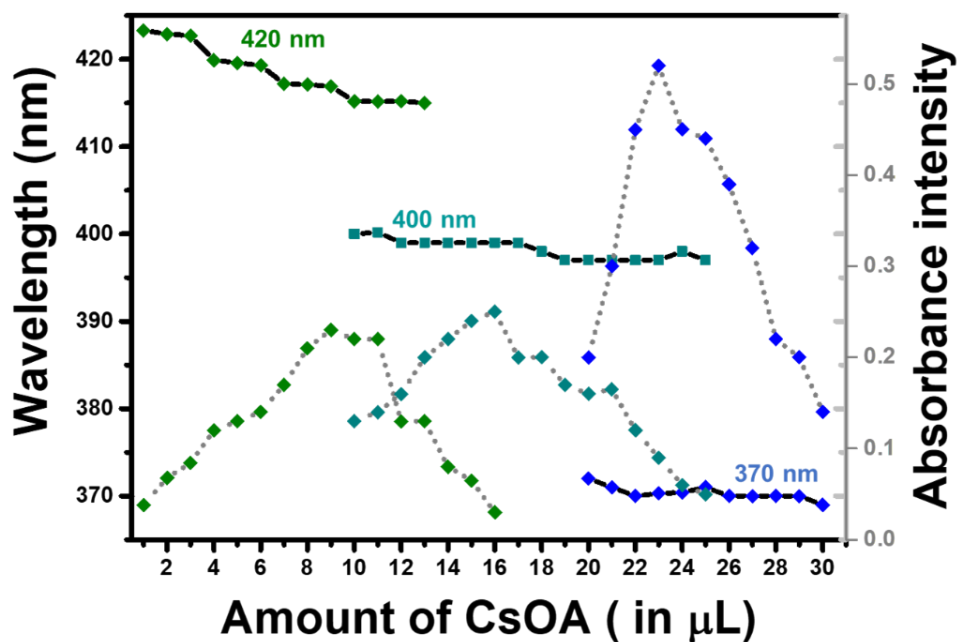


**Figure S13.** The appearance of the absorption bands at  $\approx 430$  nm, 400 nm, and 370 nm) and their gradual progress during the incremental additions (1 to 30  $\mu\text{L}$ ) of  $\text{P}_{\text{Cs-ol}}$  against 100  $\mu\text{L}$  of  $\text{P}_{\text{Pb-br}}$  in 2 mL hexane.

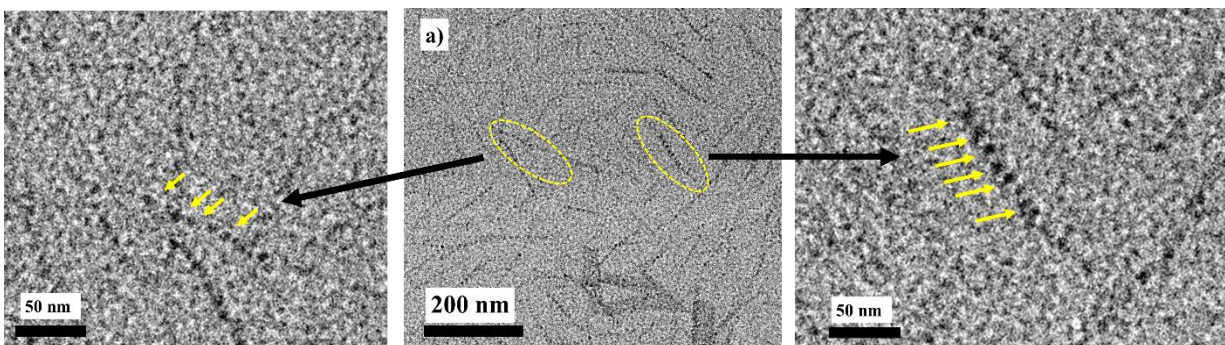


**Figure S14.** A) TEM image of the intermediate transient state whose absorption corresponds to 370 nm. Left and right TEM images are the enlarged view of the dotted yellow-colored circles. All over the grid show the presence of linear self-assembly of tiny NCs.

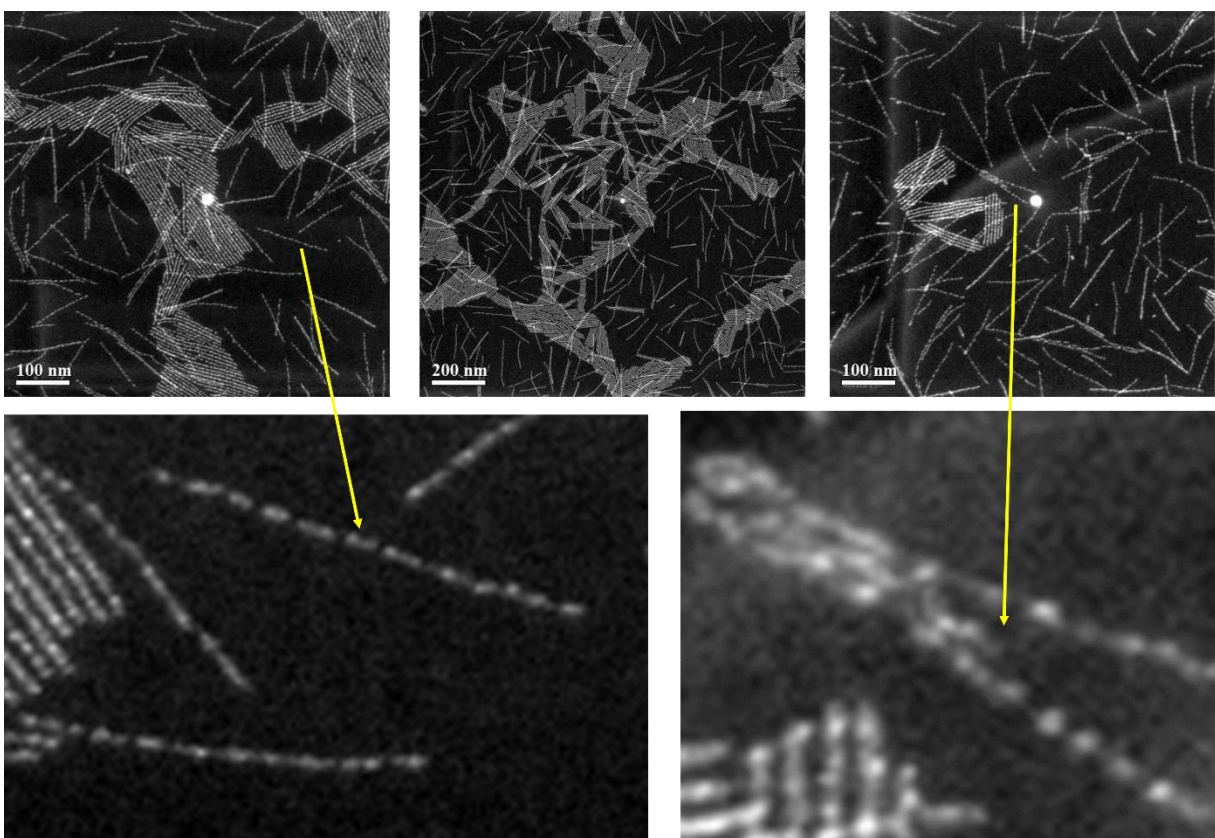
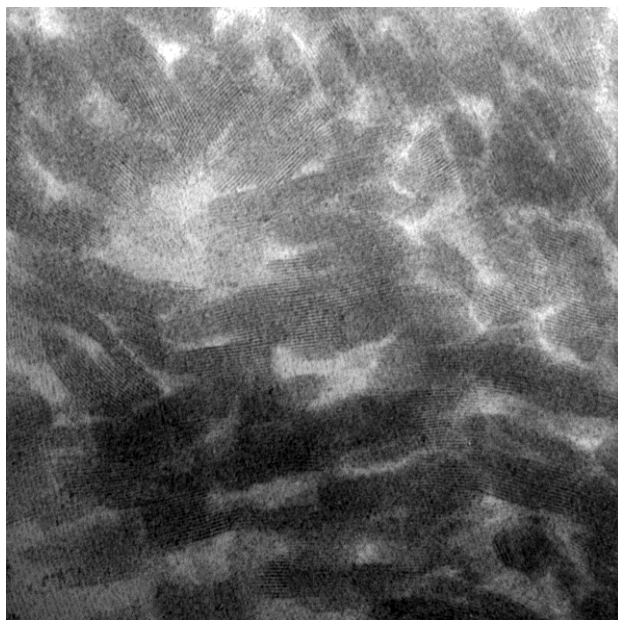
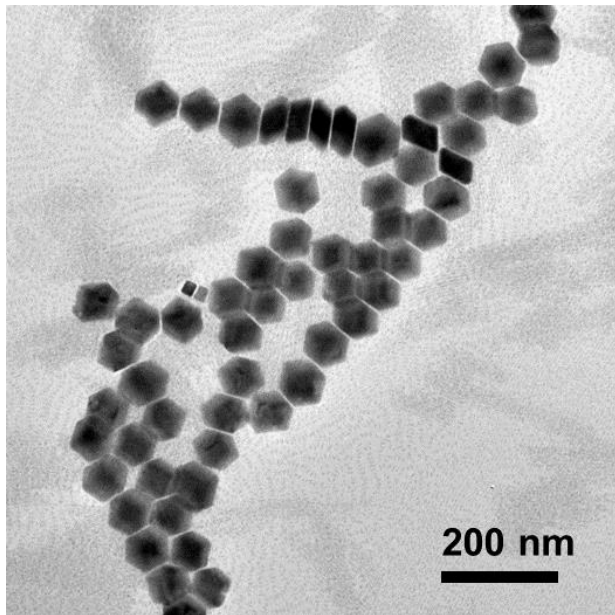


**Figure S15.** A) Representative STEM images (top row) of the intermediate transient state. Images in the bottom row show the enlarged view of the marked area of the above images. Such morphology is seen all over the grid (presence of linear self-assembly of tiny NCs which is also corresponding to the TEM data).



200 nm

**Figure S16:** Formation of CsPbBr<sub>3</sub> NBs structures formed immediately after the mixing of the precursors in the reaction condition at  $\delta_1$ .



200 nm

**Figure S17.** TEM image composed of CsPbBr<sub>3</sub> nanoplatelets and 100 nm Cs<sub>4</sub>PbBr<sub>6</sub> NCs prepared at the lower  $\delta_2$  region



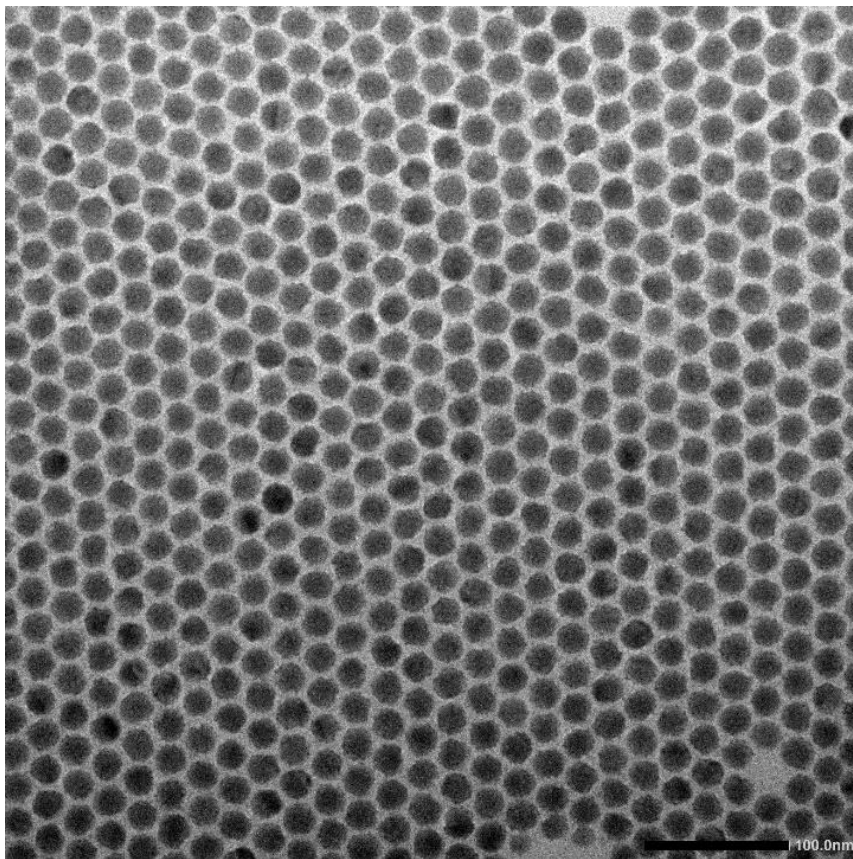


**Figure S18:** Cs<sub>4</sub>PbBr<sub>6</sub> NCs are highly monodisperse, and they form large self-assembled monolayers of hexagonally packed sheets prepared at higher  $\delta_2$  regions.

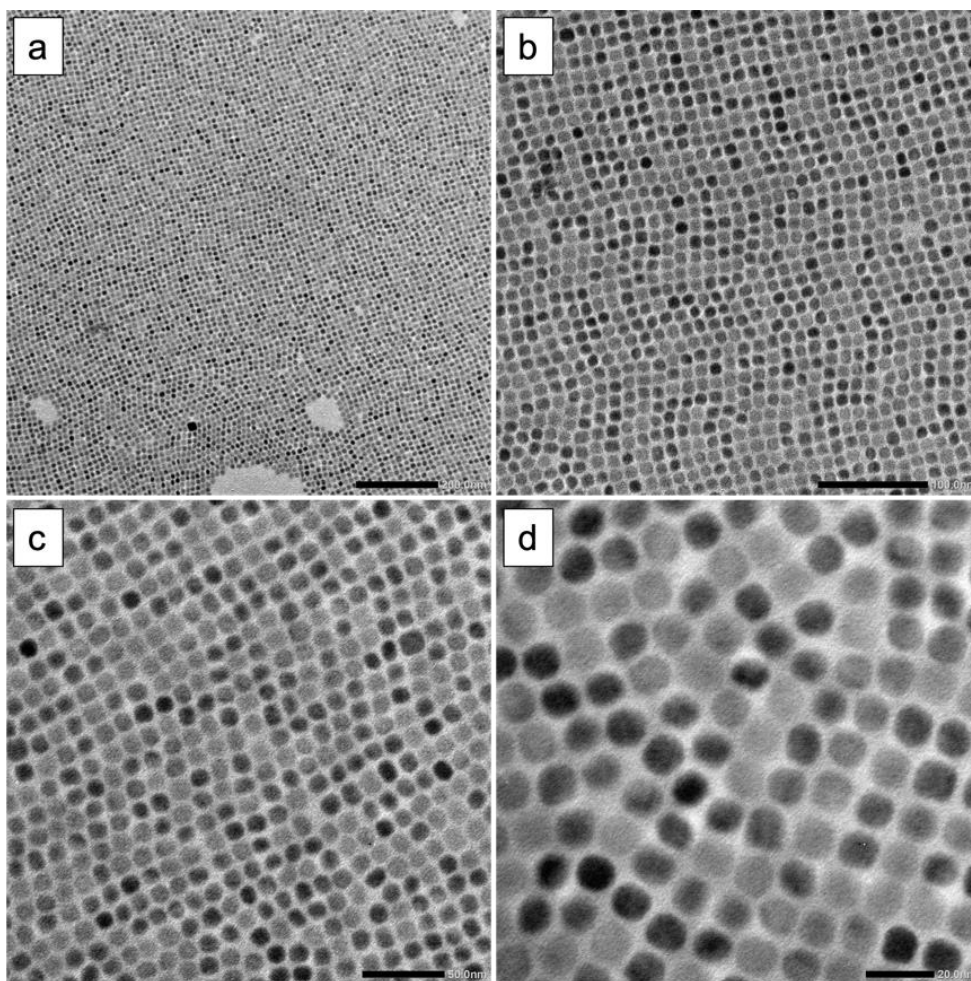


**Figure S19.** The reaction solution made at the condition of  $\delta_2$ - $\delta_3$  containing CsBr and  $\text{Cs}_4\text{PbBr}_6$  NCs underwent self-assembly upon evaporating the sample on the TEM grid. Scale bars of a, b, c, and d correspond to 200 nm, 100 nm, 50 nm, and 20 nm, respectively.

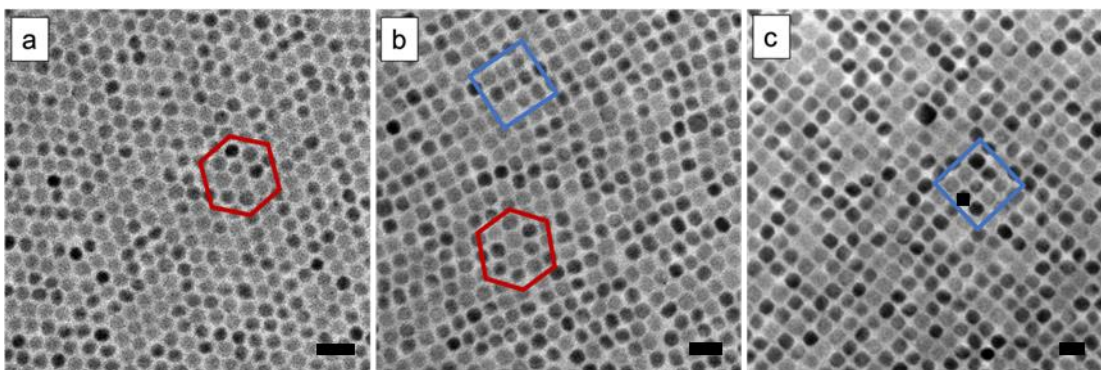


**Figure S20.** TEM images of the NCs with two different packings (hexagonal close packing, HCP, and cubic close packing, CCP) while the reaction condition was transferring from  $\delta_2$  to  $\delta_3$ . Scale bars in all the images correspond to 20 nm.

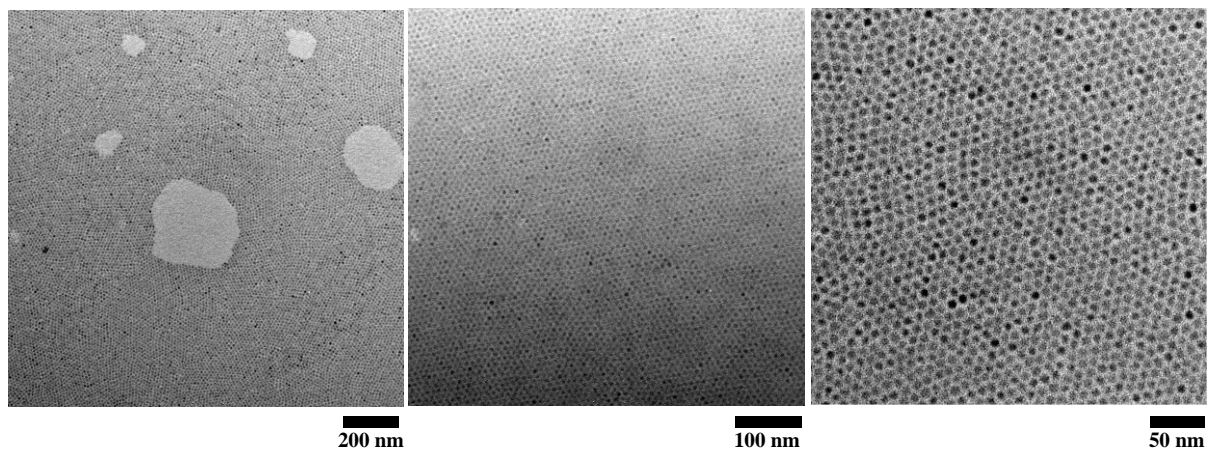


**Figure S21:** Formation of Cs<sub>4</sub>PbBr<sub>6</sub> NCs formed immediately after the mixing of the precursors at the  $\delta_2$  region.

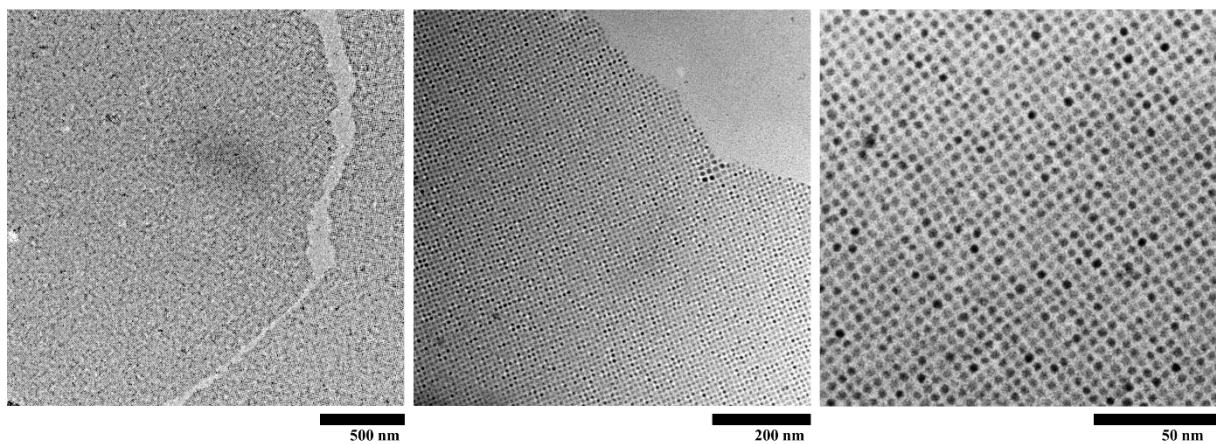


**Figure S22** The formation of CsBr NCs formed immediately after the mixing of the precursors in the reaction condition at  $\delta_3$ .

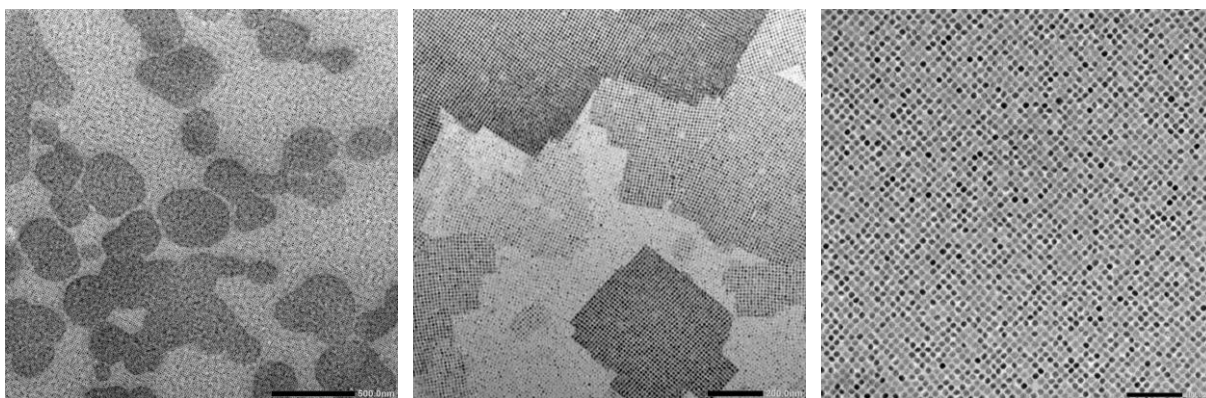


**Figure S23.** Spherical CsBr NCs prepared in lower  $\delta_3$  condition, readily undergoing square packed assembly on TEM grids into the 200 nm to 1  $\mu\text{m}$  square-shaped sheets. Scale bars from the left image to the right are 500 nm, 200 nm, and 100 nm respectively.

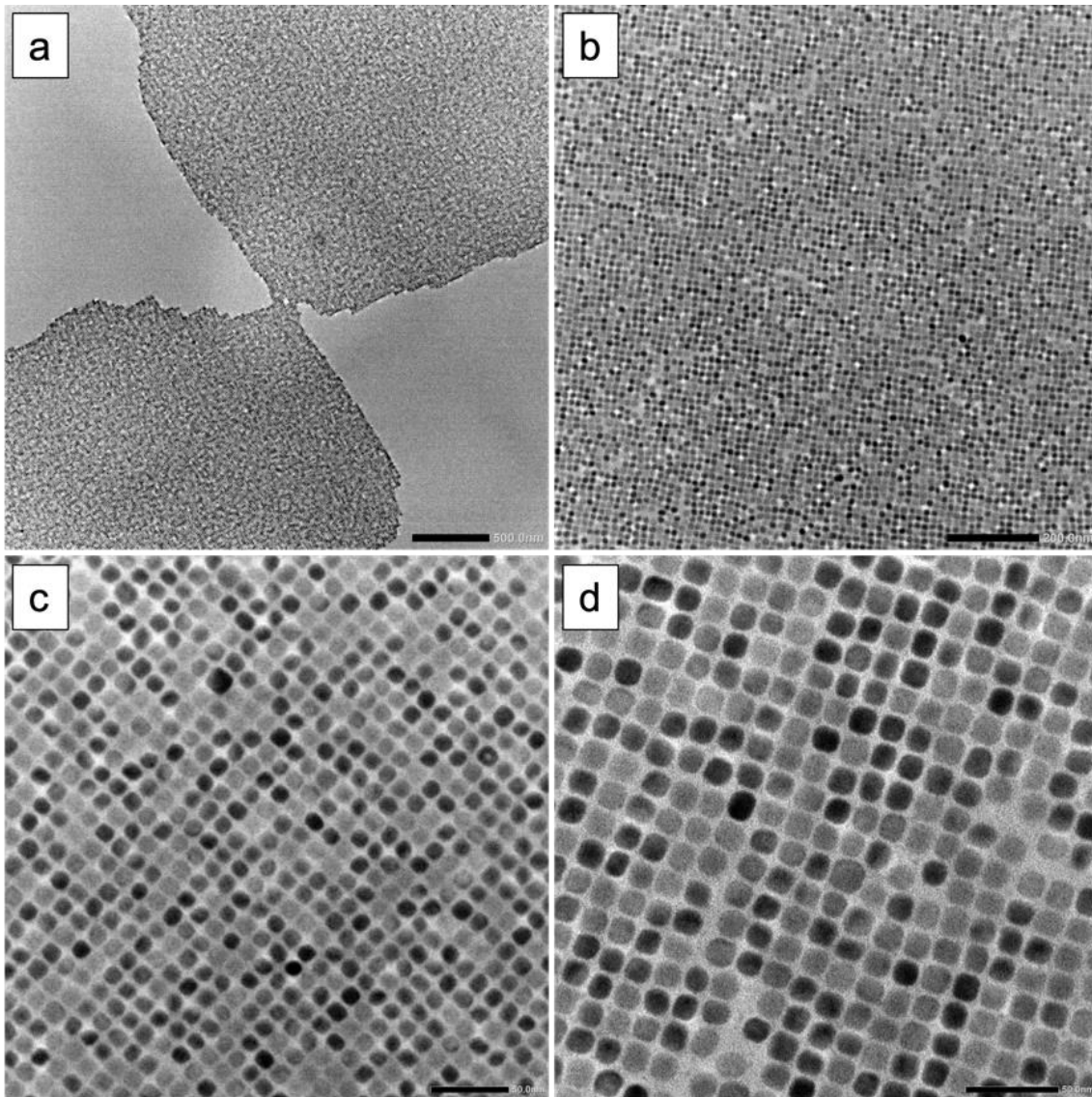


**Figure S24.** The reaction solution made under the condition at moderate  $\delta_3$  containing CsBr nanocubes underwent self-assembly upon evaporating the sample on the TEM grid. Scale bars of a, b, c, and d are 500 nm, 200 nm, 50 nm, and 50 nm respectively.

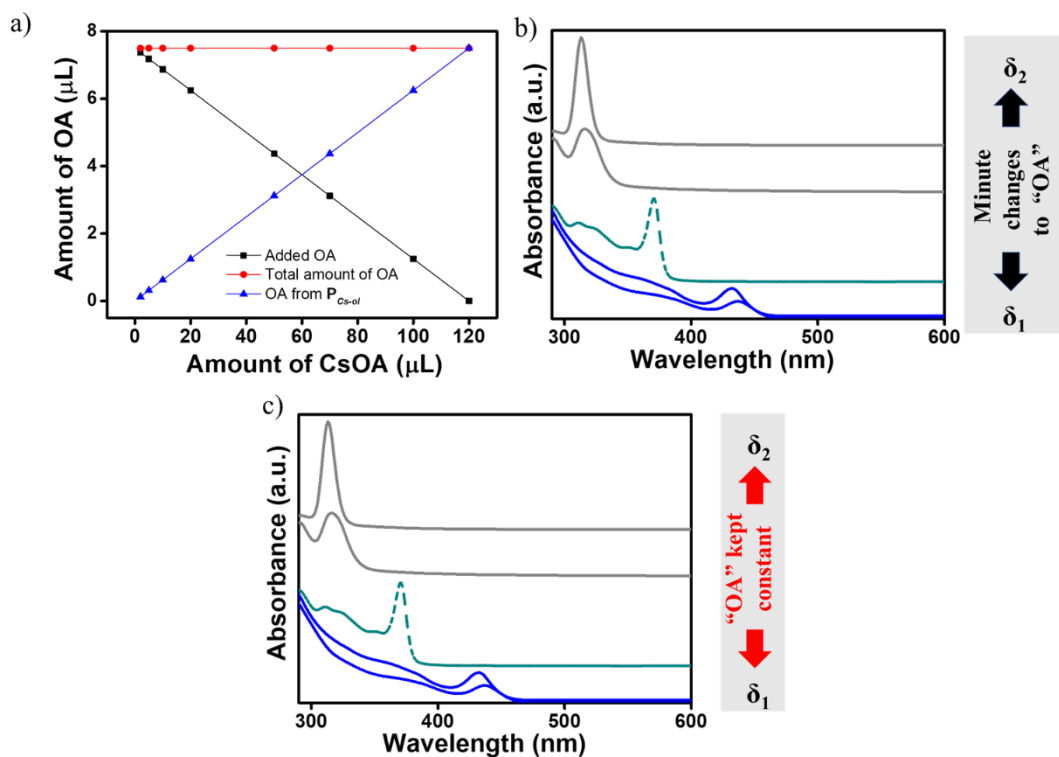


**Figure S25.** a) Amount of OA added into the reaction. i) OA from  $\text{P}_{\text{Cs-ol}}$  indicates, the amount of OA added to the reaction from the pristine  $\text{P}_{\text{Cs-ol}}$  precursor, which is rising with the increase from  $\delta_1$  to  $\delta_2$ . ii) the amount of additional OA (black) in order to maintain the constant amount of OA (red) from  $\delta_1$  to  $\delta_2$ . Corresponding absorption profiles are presented in b and c respectively. Basically, in this reaction window, the tiny amounts of OA dose do not influence the crystal phases of the final reaction products.

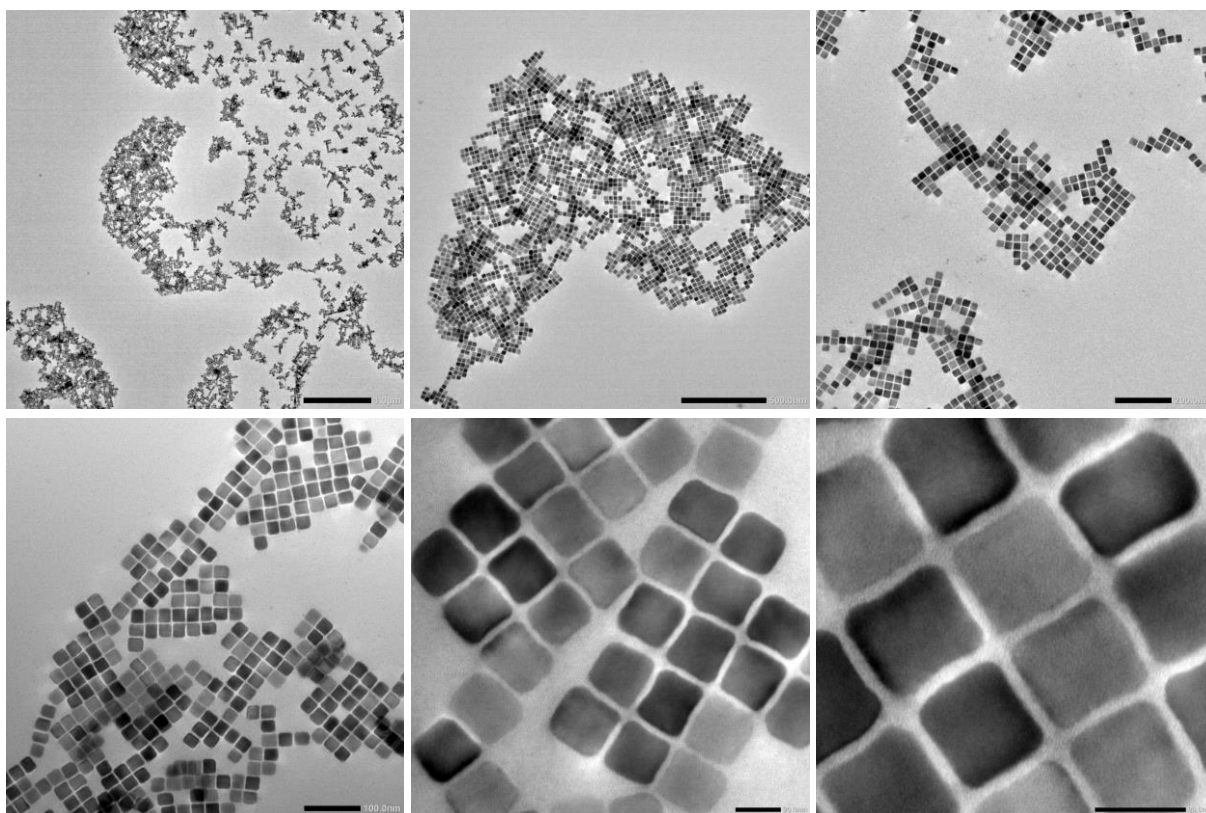


**Figure S26.** Sharp-edged CsBr nanocubes synthesized in the moderate  $\delta_3$  region in the presence of 1  $\mu\text{L}$  excess OA. Scale bars are 1  $\mu\text{m}$ , 500 nm, 200 nm, 100 nm, 20 nm and 20 nm, respectively.

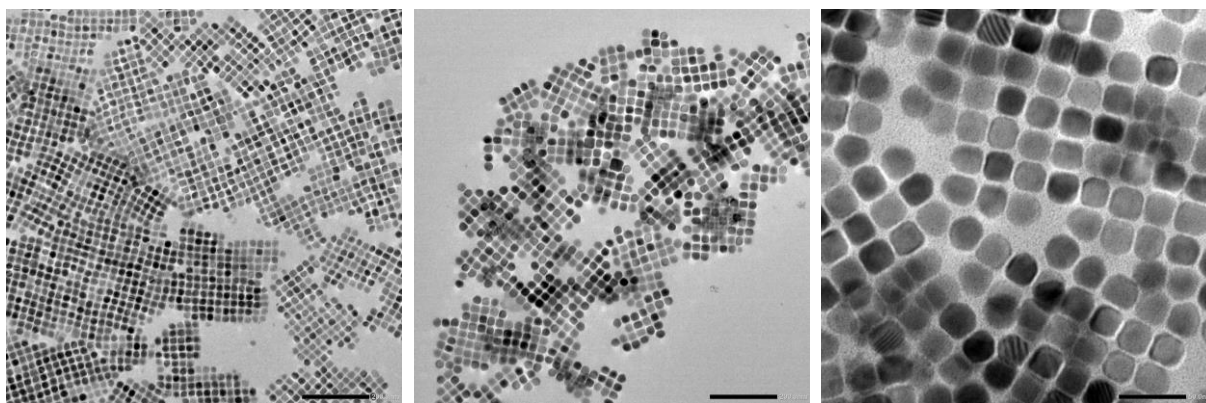


**Figure S27.** Round-edged CsBr nanocubes synthesized at the moderate  $\delta_3$  region in the presence of 1  $\mu\text{L}$  excess OLAM. Scale bars are 200 nm, 200 nm and 50 nm, respectively.

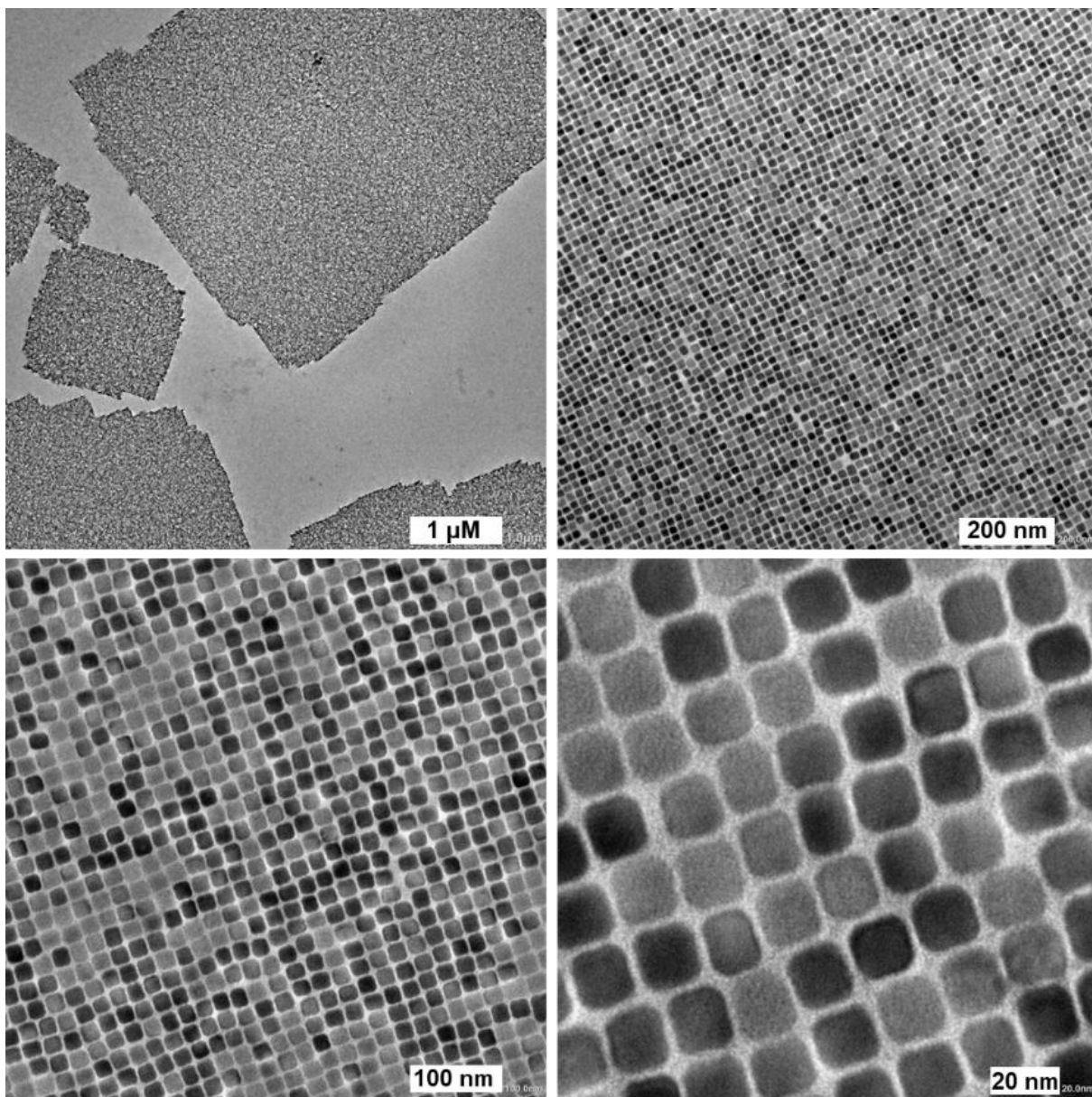


**Figure S28.** The reaction solution made at the condition at  $\delta_3$  containing CsBr nanocubes underwent self-assembly upon evaporating the sample on the TEM grid.



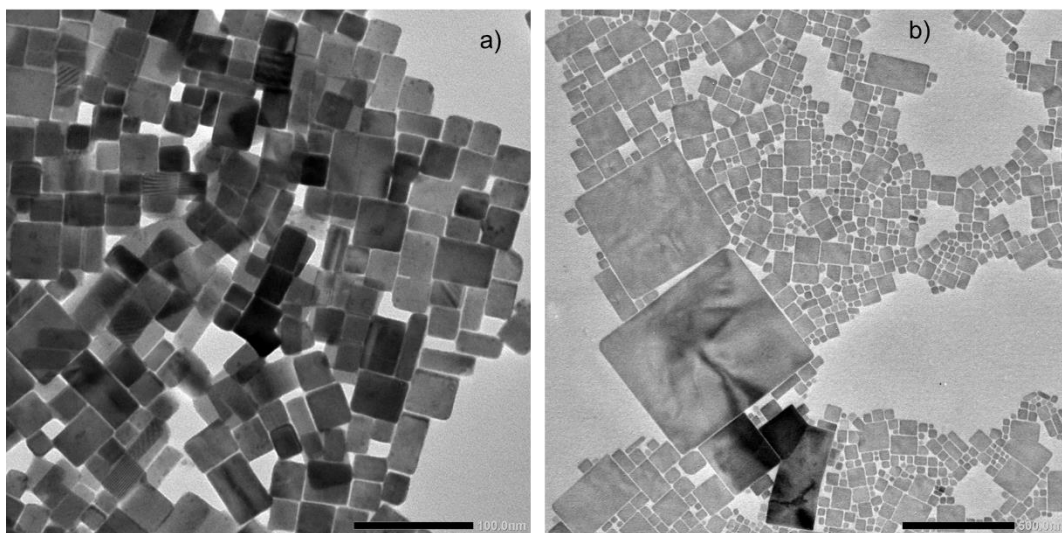


**Figure S29.** TEM images of the reaction solution prepared at the higher  $\delta_3$  region. a)  $250 \mu\text{L}$  of  $\text{P}_{\text{Cs-ol}}$  and b) beyond  $250 \mu\text{L}$  of  $\text{P}_{\text{Cs-ol}}$  against  $\text{P}_{\text{Pb-br}}$ , show the presence of larger CsBr nanocubes.

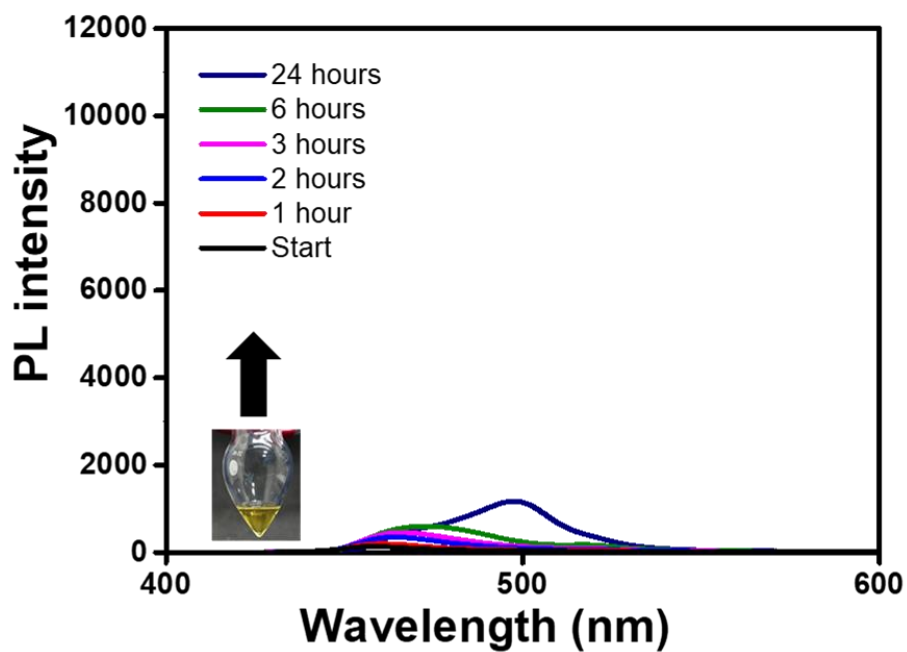


**Figure S30.** PL emission spectrum of reaction in the region of NBs collected by mixing the precursors in the absence of reaction solvent (appropriate dilution), hexane. Note that there is solvent (ODE) present in the precursor solution. PL emission of the reaction progress at 1h, 2h, 3h, 6h, and 24 h. Note that the PL intensities are 10 times lower than that of the regular synthetic conditions given in S31.

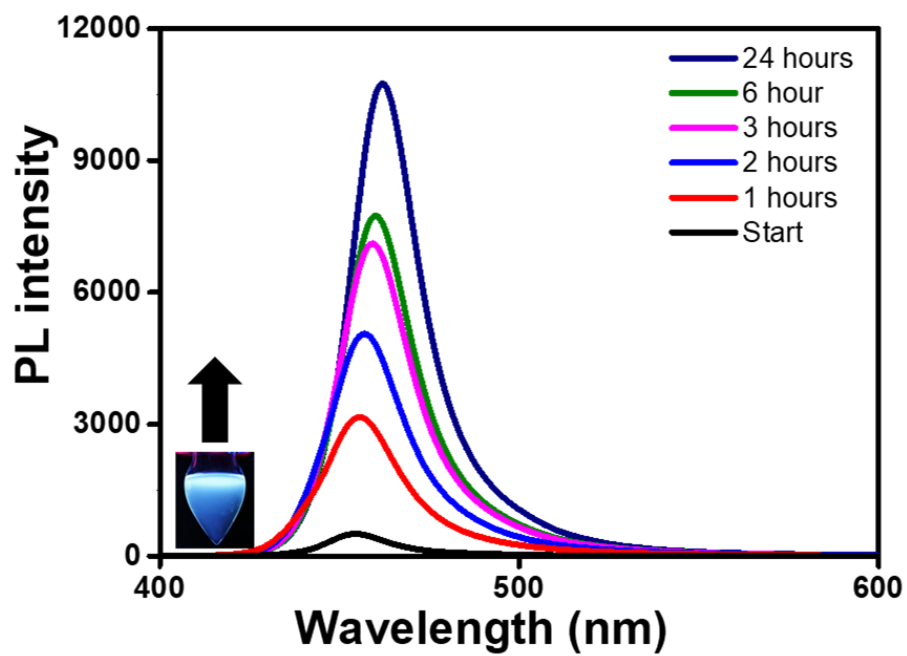


**Figure S31.** PL emission spectrum of reaction in the region of NBs collected with appropriate dilute condition (addition of  $7\mu\text{L P}_{cs-ol}$  to  $100\mu\text{L P}_{pb-br}$  in 2 mL hexane). PL spectra show the reaction progress at 1 h, 2 h, 3 h, 6 h, and 24 h.

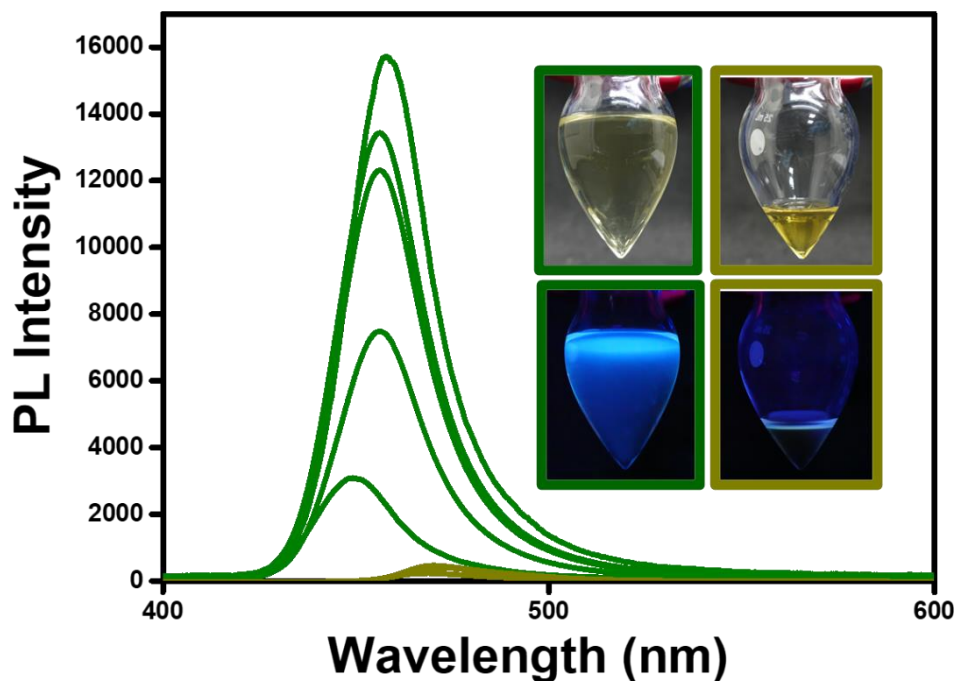


**Figure S32.** PL emission spectra of NBs collected at two different constant concentrations during the reaction progress over 24 h. The green traces indicate the PL emission spectra from reaction solutions during the reaction progress at 1h, 2h, 3h, 6h, and 24 hours. The dark yellow indicates the PL emission spectra of concentrated samples at the time intervals of 1.5 h, 2.4 h, 3.5 h, and 6.5 h and 20 h of the reaction, showing the quenching of PL emission.

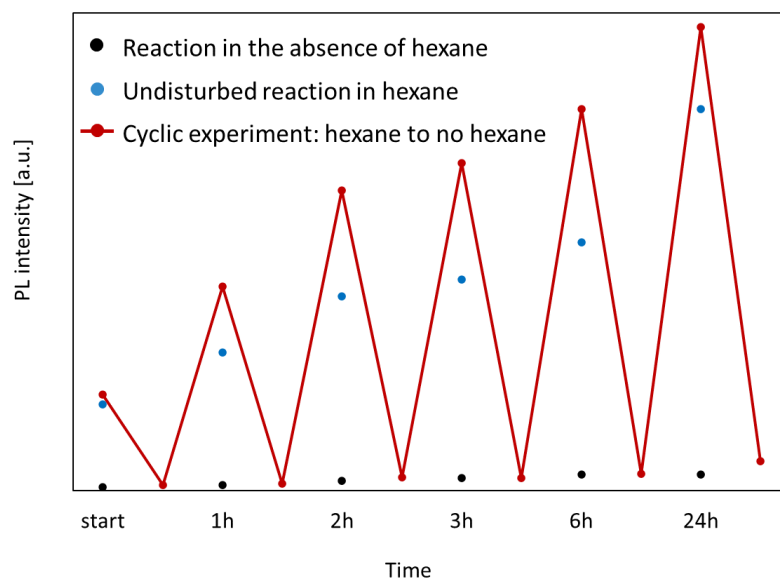


**Figure S33.** PL emission spectrum of NBs collected at two different constant concentrations during the reaction progress over 24 h. The rising red lines indicate original solutions during reaction progress at 1 h, 2 h, 3 h, 6 h, and 24 h. Falling red lines represent the quenching of PL intensity between the reaction progress via subjecting to solvent evaporation, thereby increasing the concentration. PL emission results of a sample without hexane solvent (black dots) and with hexane undisturbed (blue dots) are shown as control.

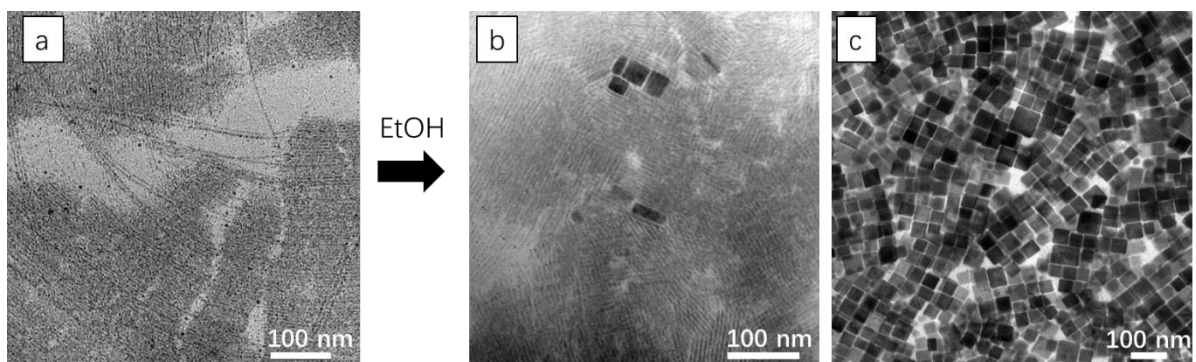


**Figure S34.** TEM images of the reaction conducted at the  $\delta_1$  region show the presence of CsPbBr<sub>3</sub> NCs (a) and the respective CsPbBr<sub>3</sub> nanoplatelets (b) and CsPbBr<sub>3</sub> nanocube structures (c) formed at the addition of 10  $\mu$ L and 100  $\mu$ L addition of EtOH to the reaction (a).